PARTICLE SIZE DISTRBUTION IN A HYPERVELOCITY IMPACT EXPERIMENT ON DRY SANDSTONE.
E. Buhl[1,2], M. H. Poelchau[2], G. Dresen[1] and T. Kenkmann[2], [1]German Research Centre for Geosciences - GFZ Potsdam, Germany (buhl@gfz-potsdam.de), [2]Institute for Earth and Environmental Sciences, University of Freiburg, Germany.

Introduction: The particle size distribution (PSD) is a commonly used parameter to describe the deformation-induced fragmentation in faulted rocks. It has been shown that resulting particle sizes are properly described by a fractal size distribution [1]. This characterization is described by the relationship of particle frequency versus particle size

$$N(d) \sim d^D$$

where $N(d)$ is the number of particles smaller that diameter d, and D is the "fractal dimension" (D-value). This method has frequently been used to describe natural fault zones, e.g. [2] and deformation experiments, e.g. [3]. PSD reported for impact events are sparse. D-values of PSDs for natural impacts [4,5] and impact experiments [6,7] have been reported to range between 1.2-1.8 and 1.4-1.7, respectively. For the first time here we show the systematic distribution of the PSD in the subsurface of an experimental impact crater.

Experiments and Results: The investigated experiment was performed in the framework of the MEMIN research group [8] at the two-stage acceleration facilities of the Fraunhofer Ernst-Mach-Institute (EMI) in Freiburg, Germany. A 20 cm cube of quartz-rich sandstone (*Seeberger Sandstein*) was impacted by a 2.5 mm steel sphere at 4.8 km/s [9]. The resulting crater cavity has a diameter of 5.76 cm a depth of 11.0 mm. For the investigation the crater was impregnated with low viscosity epoxy and the block was cut in halves. For microanalysis thin sections were prepared along a cross-section through the crater subsurface. The thin section micro-analysis was conducted by means of a Zeiss Leo 1525 field emission scanning electron microscope (FE-SEM) in backscattered electron (BSE) mode (20 kV, 16 mm working distance). A succession of 20 images (400x magnification) with increasing distance from the crater floor was analyzed regarding the PSD. Each image covers an area of 660x883 µm (0.583 mm²). The automated digital image analysis software JMicrovision was used for spatial calibration and automated object extraction from the BSE photomicrographs. A gray scale threshold was used to separate the quartz particles from pore space and the clay mineral content. Area and perimeter of all detected particles were exported and used for PSD analysis. For the particle size d, the equivalent circular diameter, calculated as the diameter of a circle with the same surface area as that of the measured particle, was used. To plot the PSD the particle sizes were binned in 20 size classes. The particle size distribution in Fig. 1 is shown in log-log plots as number of particles ($N(d)$) with a diameter >d against the diameter.

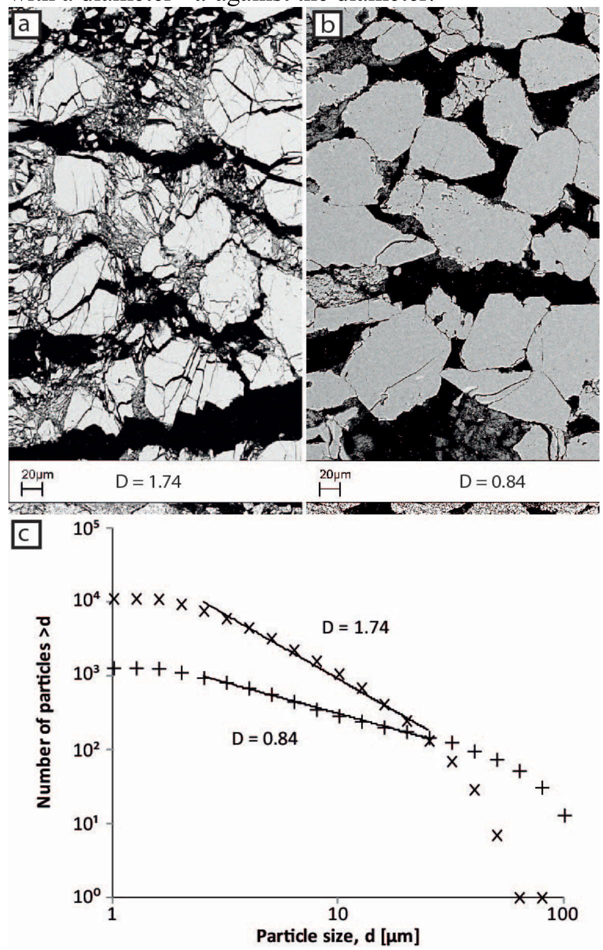

Fig. 1: BSE micrographs of fragmented sandstone and the resulting D-values. a) Pervasive comminution at the crater floor. b) Incipient fragmentation at 7.2 mm beneath the crater floor. c) Log-log diagram of particle number vs. particle size for both images. D-values are obtained by the slope of the linear logarithmic regression lines.

All obtained PSD graphs in this study can be reasonably fit with a linear function in a log-log plot over at least one order of magnitude. For this interval they can, thus, be described by the power law relationship $N(d) \sim d^D$, where D is the D-Value. As obtained from thin sections all D-values reported here are two dimensional D-values.

A microstructural description of the subsurface deformation features within the impacted sandstone is given in [10]. The distinct modes of deformation reported there are closely linked to the fracture pattern developed in the sandstone and thus with the *D*-value. As expected, more effective comminution was detected closer to the crater floor. To quantify this initial observation, a series of images beneath the crater floor was analyzed for their PSD. All obtained curves exhibit a fractal range [2] that, in all cases, covers at least one order of magnitude of particle size. A systematic decrease of the *D*-values was found with increasing distance from the crater floor (Fig. 2).

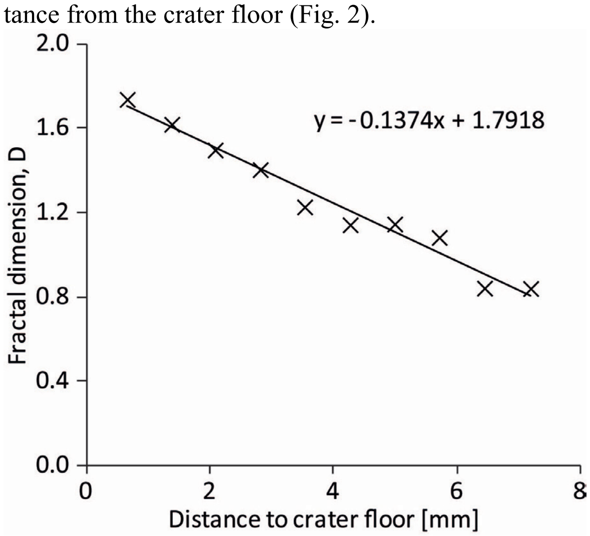

Fig. 2: *D*-values evolution with increasing depth beneath the crater floor. The trend was found to be best described as linear.

The highest *D*-value of 1.74 was found at a depth of 0.26-1.07 mm beneath the crater floor. With growing distance the *D*-values drop steadily to a value of ~0.84. All measured *D*-values and the mean distance of the depth of investigation are given in Table 1. Additionally, correlation coefficients (R^2 values) are given as a measure of the quality of the regression lines fit to the curves.

Table 1: Measured D-values and R^2 values.

Distance to crater floor [mm]	D-value	Correlation coefficient R^2
0.7	1.74	0.9842
1.4	1.62	0.9818
2.1	1.50	0.9869
2.8	1.41	0.9884
3.5	1.23	0.9918
4.3	1.14	0.9922
5.0	1.15	0.9940
5.7	1.08	0.9969
6.4	0.84	0.9996
7.2	0.84	0.9968

Discussion: Impact induced fragmentation of rock and the resulting particle size distribution may be well described by a power-law with a D-value changing with vertical distance from the crater floor. Our results for the first time show a spatial resolution of *D*-values for an impact event. Comparison with the reported data from natural impact sites and experimental impacts shows that our results cover almost all of the reported values. This means that a spatial context is necessary and should be given when *D*-values are reported. Doing so could lead to a deeper understanding of the crater geometry and post impact deformation and erosion. The obtained D-values overlap with those of tectonic fault zones. Hence D-values are not uniquely related to a specific deformation process.

Outlook: A detailed and spatially resolved analysis of the *D*-values of the ejected material from this experiment is planned. This might improve our understanding of ejecta emplacement and size distribution of space debris. We also intend to compare the fragmentation behavior of wet and dry targets.

Acknowledgments: The MEMIN research unit FOR 887 and the Projects KE 732/15-1 and DR 213/15-1 are funded by the German Research Foundation DFG.

References:

[1] Turcotte D. L. (1986) *JGR,* 91, 1921-1926 [2] Blenkinsop T. (1991) *Pure Apl. Geophys.,* 136, 60-86 [3] Marone C. and Scholz C. (1989) *J. Struct. Geol*., 11, 799-814 [4] Rousell D. H. et al. (2003) *Earth-Sci. Rev.,* 6, 147-174 [5] Key W. R. O. and Schultz R. A. (2011) *GSA Bulletin,* 123, 1161-1170 [6] Fujiwara A. et al. (1977) *Icarus,* 31, 277-288 [7] Lange M. A. et al. (1984) *Icarus,* 58, 383-395 [8] Kenkmann T. et al. (2011) *M&PS,* 46, 890-902 [9] Poelchau M. H. et al. (2013) *M&PS,* (48), in press [10] Buhl E. el al. (2013) *M&PS,* (48), in press.